Evolution of species' range and niche in changing environments

Jitka Polechová[1,*]
[1] University of Vienna, Department of Mathematics
[*] E-mail: jitka@univie.ac.at

Abstract

What determines the limits to adaptation and to a species' range is a fundamental question, especially relevant in the context of current rapid environmental change. Yet, to date, no predictive theory incorporates the feedback between ecology and evolution while accounting for the evolution of genetic variance under selection, mutation, dispersal, and genetic drift. This study outlines a comprehensive theory showing that under joint evolutionary and population dynamics, the limits of adaptation are fundamentally determined by the three measurable parameters: i) the effective environmental gradient, ii) the effective rate of temporal change, and iii) the neighbourhood size, which represents the local population size accessible via dispersal. Dispersal across heterogeneous environments supports higher local genetic variance, facilitating adaptation to a faster temporal change. However, local diversity is depleted by genetic drift, which is measured by the inverse of neighbourhood size. Extending earlier predictions in stable environments, I use scaling arguments to derive a generalized expansion threshold – a tipping point where adaptation fails and the species' range can no longer expand. Beyond this threshold, species' ranges also tend to fragment, particularly when temporal change incurs a high fitness cost. The onset of fragmentation is rapid and associated with a loss of genetic variance. The theory not only identifies new phenomena but also establishes a fundamental relationship between these core measurable parameters. It provides a predictive framework for understanding species' range and niche limits while advancing the theoretical foundations for assessing population resilience of spatially structured populations under unprecedented environmental change.

keywords: adaptation, environmental change, range margin, species' range, geographic range, trailing edge, leading edge, ecological niche, evolution, expansion (10)

Introduction

As environments change over time, species' ranges may shift, expand or contract while their ecological niches change through adaptation. These evolutionary and ecological processes are interconnected: while population growth is determined by the mean fitness of the population, the rate of adaptation depends on the genetic variance, the strength of natural selection and the population size (*via* genetic drift) (Haldane, 1957; Lande, 1976; Paixão & Barton, 2016). Even considering a single, focal species, the interaction between demographic and evolutionary dynamics in spatially and temporally varying environments is complex and thus difficult to predict. Theoretical progress has been made by assuming genetic variance is fixed (Aguilée *et al.*, 2016; Chevin *et al.*, 2010; Pease *et al.*, 1989; Polechová *et al.*, 2009) or assuming population subdivision but no explicit space, particularly considering evolutionary rescue (Gomulkiewicz & Holt, 1995; Uecker *et al.*, 2014). Although evolution of genetic variance in response to the variable environment can profoundly change the outcome, it remains largely ignored in the current predictive eco-evolutionary theory.

In spatially structured populations, a substantial proportion of genetic variance can be maintained by gene flow across heterogeneous environments: with increasing environmental gradient and dispersal, the relative contribution of mutation-selection balance to genetic variance diminishes. Furthermore, the interaction between the effects of spatial and temporal variability on the genetic variance can have complex effect on the rate of adaptation and the probability of evolutionary rescue (Benning *et al.*, 2022; Czuppon *et al.*, 2021; Fouqueau & Polechová, 2024; Holt *et al.*, 2004, 2022; Osmond & Klausmeier, 2017; Sexton *et al.*, 2009; Tomasini & Peischl, 2022). Yet, studies focusing on eco-evolutionary dynamics in jointly spatially and temporally varying environments, which do not assume that genetic variance is fixed (while considering more than 1-2 loci), remain rare as the increasing complexity hinders the general interpretation of the results. To date, predictive quantitative results regarding range and niche and evolution in spatially and temporally variable environments are lacking.

One of the key factors influencing species' range dynamics and the resilience of populations facing rapid environmental change is dispersal (Débarre *et al.*, 2013; Holt & Gomulkiewicz, 1997). The role of population subdivision and dispersal is central to Wright's 1932 shifting balance theory but the impact of dispersal and gene flow is complex even on smooth fitness landscapes. Writing about fundamental limits to adaptation and the apparent stability of species' borders, Haldane (1956) introduced the idea of the feedback between asymmetric gene flow and reduction of local population size as a possible driving force behind a stable margin of a species' range; an example of migration meltdown (Ronce & Kirkpatrick, 2001) due to "swamping" gene flow. However, increasing gene flow does not necessarily hinder adaptation across environmental gradients. Dispersal across heterogenous environments elevates genetic variance (Felsenstein, 1976; Hedrick, 1986), which, while increasing the standing load (fitness cost of genetic variance), also accelerates the rate of adaptation and reduces lag load (fitness cost of a distance of a trait mean from an optimum; Lande & Shannon 1996).

Dispersal also has an important effect on stochasticity: it enlarges the neighbourhood size, thereby decreasing the power of genetic drift relative to selection. The neighbourhood size, defined by Wright (1943; 1946), measures the weakness of genetic drift in populations distributed across continuous space and can be thought of as a population within the standard deviation of dispersal distance σ. In two dimensions with diffusive dispersal, this corresponds to the population $\mathcal{N} = 2\pi\sigma^2 N$ within the area of a circle with a diameter σ and local population density N – and can be thought of as a local mating pool. Interestingly, although sufficient neighborhood size is critical for the maintenance of adaptive diversity across space (Charlesworth *et al.*, 2003; Nagylaki, 1978b; Polechová & Barton, 2011), it is currently almost never explicitly considered in conservation guidelines (though see Lande *et al.* 1987; Vekemans & Hardy 2004). Despite a growing understanding that increasing dispersal and gene flow may enhance the resilience of populations, especially under changing environments (Sexton *et al.*, 2024), the importance of population structure,

and neighbourhood size in particular, remains neglected.

What causes the species' niche and range margins is not only a fundamental theoretical question but also directly affects how we assess the resilience of natural populations in current and future environments. Yet, despite the urgent need for predictive theory in times of accelerated climate change, the assumptions of current eco-evolutionary theory remain rather restrictive. In this study I provide testable predictions on limits to adaptation in changing environments, which arise from the feedback between selection, genetic drift and population dynamics.

Model and methodology summary

The core features of the model are the eco-evolutionary feedback *via* coupling between fitness and population growth, inclusion of both genetic and demographic stochasticity and a quantitative genetic model where both the trait mean and its variance evolve. The effect of environment (biotic and abotic) is condensed to a gradient in an optimum value of a trait of the focal species. The optimum changes through time along one of the two spatial coordinates: an example could be a spatial gradient in optimal flowering time, changing with altitude (or latitude) and time. Both range and niche shifts are possible: gradient of habitats is accessible via dispersal and the selected trait – including its variance – can evolve freely.

Individual fitness depends both on local density and the distance of the trait from the environmental optimum. Population growth is given by the mean fitness, which reflects the local density and phenotypic distance for the optimum. Selection is hard (*sensu* Christiansen 1975): i.e., the locally attainable density ("carrying capacity") declines with maladaptation. An additive quantitative trait that influences adaptation to the environment is determined by a large number of loci with exponentially distributed effects α. There is free recombination but there are no differences between sexes; for simplicity, individuals are assumed to be hermaphroditic and haploid. Thus, there are no dominance effects; yet there is epistasis as the fitness effect of each allele depends on other allele frequencies via the trait mean. Dispersal distances are normally distributed, independent of fitness and do not evolve through time. The model is written both as an individual-based discrete-time simulation and as an analytical continuous-time model of joint evolutionary and population dynamics.

The dynamics of this fairly complex model are elucidated with the help of the following steps: First, the continuous-time model is rescaled in terms of dimensionless parameters. This reduces the system's dimensions, simplifying the analysis and facilitating future testing of predictions. Second, the outcomes of the individual-based model are compared to known analytical expectations of simpler systems: namely to the deterministic equilibria and the predictions of a phenotypic model with fixed genetic variance. An illustrative example of the individual-based model is given at Fig. S1.

Results

This model of species' range and niche dynamics has over ten parameters, which arise from coupling the classic formalizations of evolutionary and ecological dynamics. Fortunately, there is a rescaling which both reduces the (apparent) dimensionality of the problem and facilitates interpretation. Upon nondimensionalization, we obtain five dimensionless parameters which describe the core system (extending from Kirkpatrick & Barton 1997; Polechová 2018; Polechová *et al.* 2009). The first parameter measures the effective rate of change of the optimum through time: $k^* = k / \sqrt{V_s\, r^{*3}}$ relative to the strength of stabilising selection V_s and the rate r^* at which the population returns to its demographic equilibrium, where k is the rate of temporal change. The second parameter $B = b\,\sigma/(\sqrt{2V_s}\, r^*)$ describes the effective steepness of the environmental gradient b across space x in terms of the expected reduction in

fitness due to dispersal σ. The third parameter is the neighbourhood size $\mathcal{N} = 2\pi\sigma^2 N$ which describes the population attainable within a generation's dispersal and measures the weakness of genetic drift on local scales; N is the local population density. (There is a 2 rather than 4 as the model is haploid – for a diploid organism, neighbourhood size doubles.) The fourth parameter is the strength of selection $s \equiv \alpha^2/V_s$ relative to the rate of return of population to a demographic equilibrium s/r^* and finally the fifth is the scaled mutation rate μ/r^*. Further details on the model and its scaling are given in the Methods.

The rate of adaptation increases with the product of selection gradient and additive genetic variance (Fisher, 1930; Lande, 1976). The genetic variance itself increases with the effective environmental gradient B such that in the absence of stochastic and demographic effects, the scaled genetic variance is $A = V_G/(r^* V_s) = \sqrt{2}B$ (Barton, 2001). We might thus expect that with increasing heterogeneity of the environment, measured by the effective environmental gradient B, the genetic variance will steadily rise and thus support adaptation to ever-increasing temporal change k^*: yet, this would only be true in infinitely large populations. Increasing spatial heterogeneity aids adaptation until the load due to genetic variance becomes too large: coupling between evolution and demography will eventually incur cost high enough so that the population will go extinct. Furthermore, long before the deterministic extinction, genetic and demographic stochasticity reshape the dynamics.

The influence of the effective environmental gradient B and the effective rate of temporal change k^* on the rate of species' range and niche expansion is demonstrated in Fig. 1. It shows that there is a fundamental bound to species' range expansion at $k^* = \sqrt{2}A = 2B$ (red dashed line), which extends from the threshold derived by Lande & Shannon (1996) for a given genetic variance in absence of spatial structure. The depicted line uses the predicted deterministic genetic variance maintained by gene flow across heterogeneous environments. Yet adaptation to temporal change fails considerably before this upper bound is reached. This is because genetic drift depletes genetic variance when neighbourhood size $\mathcal{N}$ is small, which hinders adaptation. In the absence of temporal change, the limit where continuous adaptation to environmental gradients is possible is given by $\mathcal{N} \gtrapprox 6.3\,B + 0.56$ (Polechová, 2018). Below this limit, genetic drift is too strong relative to selection for stable clines to form. This threshold is depicted by a green diamond ♦ in Fig. 1.

When the optimum changes through time, this limit to adaptation changes. A moving optimum induces a lag load, which incurs further demographic cost, thus lowering the neighbourhood size: the increase in genetic drift then reduces genetic variance. The expansion threshold in changing environments is determined jointly by the effective environmental gradient B, the neighbourhood size $\mathcal{N}$ and the effective rate of temporal change k^*. Its approximate form, given by $k_c^* = 2B(1 - 8/\mathcal{N})\sqrt{1 - (6.3B + 0.56)(\sqrt{2}B + 2h^2)/(2h^2\mathcal{N})}$, is shown by a green curve in Fig. 1; $h^2 \equiv V_G/V_P$ gives the narrow-sense heritability for the additive trait. Note that this approximate threshold only depends on the balance of k^*, B and $\mathcal{N}$. It outlines the scaling for the transition between expanding well adapted populations with variance maintained by staggered clines in allele frequencies *vs.* collapsing populations where genetic drift overwhelms selection and the variance is depleted. In contrast, rates of adaptation and range expansion would also depend on the mutational input μ/r^* and the selection strength per locus, s/r^*. The robustness of the threshold to selection per locus $s \equiv \alpha^2/V_s$ is demonstrated at Fig. S3.

The estimate of the generalised expansion threshold utilises the expected increase of demographic loads due to k^* and B as well as the reduction of genetic variance due to genetic drift. In two-dimensional habitats, the decrease of genetic variance with drift can be described as $V_G \approx V_{G,det}(1-8/\mathcal{N})$ for $\mathcal{N} > 8$, where $V_{G,det} = b\,\sigma\sqrt{V_s} + V_m$ gives the deterministic variance (Barton, 2001) – see Fig. 2. This estimate assumes that the reduction of genetic variance in two dimensions takes the same form as in one dimension (Polechová & Barton, 2011), with the dimension-appropriate neighbourhood size, and the constant of 8 is numerically fitted. When the optimum changes in time as well as in

space, the selection arising from the distance between the trait mean will favour clines in additional allele frequencies which then shift through space. The resulting increase of variance is thus stable over longer time scales; quantitive analysis of the evolution of variance in both spatially and temporally variable environments will be subject of a forthcoming paper.

Increasing neighbourhood size promotes adaptation by mitigating genetic drift and supporting adaptation to steeper environmental gradients B and faster temporal change k^*.The change of the threshold with neighbourhood size, while keeping the total population size approximately constant by scaling the neutral width of the habitat inversely with local carrying capacity, is shown in Figures S4 and S5. Neighbourhood size also increases with dispersal but so does the effective environmental gradient B. Yet, in two dimensions, neighbourhood size $\mathcal{N} = 2\pi\sigma^2 N$ increases with the square of dispersal distance σ^2, while the effective gradient $B = b\,\sigma/(\sqrt{2V_s}\,r^*)$ increases only linearly. Although there is a fitness cost associated with a rising effective environmental gradient B as dispersal increases, it is smaller than the advantage arising from increasing neighbourhood size when genetic drift is strong. Fig. S6 demonstrates that when genetic drift is strong, the benefits of reducing genetic drift *via* increased dispersal outweigh the costs associated with a rising dispersal load.

A notable phenomenon arising beyond the expansion threshold as environment changes through time is range fragmentation (see Fig. 1 D). Fragmentation is rapid and occurs in both the physical space and in the trait (niche) space (Fig. S2). It stems from the inability to sustain continuous adaptation when genetic drift is strong: clines in allele frequencies, which steepen due to genetic drift, become unstable. As fewer (and steeper) clines are maintained, local genetic variance declines. With variance lower than the threshold consistent with continuous adaptation, population fragments as genetic variances plummets. With very low adaptive variance, fragmented populations can only persist by tracking the old habitat in space and even if this habitat is available, tend to slowly decline in size: the resilience of the fragmented populations is low due to their low adaptability coupled with high demographic stochasticity. Fragmentation can also occur in the absence of temporal change, where it is facilitated by higher demographic stochasticity (Polechová, 2018). When environments change in time faster than the k_c^* threshold, fragmentation associated with fast depletion of variance is observed even for larger neighbourhood sizes (see Fig. 1).

Last, I briefly explore the effect of adaptive phenotypic plasticity. Fig. S7 demonstrates that adaptive phenotypic plasticity does not extend the range of survivable rates of temporal change in the same way as it does for spatial variability. Adaptive phenotypic plasticity implies that the expressed trait z is closer to the optimum θ than expected based on its genetic basis alone, $(z - \theta) \rightarrow (1 - \mathfrak{p})\,(z - \theta)$, where $\mathfrak{p}$ denotes adaptive plasticity. This means that the spatial gradient B appears shallower by $1 - \mathfrak{p}$. While this reduces demographic load and lowers the impact of genetic drift, it also diminishes the increase in genetic variance due to spatial variability. Thus, when genetic variance evolves in response to the effective environmental gradient, the effect of plasticity on adaptation to a steady temporal change largely cancel out. This finding contrasts with predictions assuming fixed genetic variance in he selected trait is fixed, where the benefits of plasticity in response to variation in time and space are equivalent (Chevin *et al.*, 2010; King & Hadfield, 2019).

Discussion

This theory gives quantitative predictions concerning species' range limits, adaptation and resilience, and highlights both the importance of spatial variability for temporal adaptation (Alberto *et al.*, 2013; Garcia Castillo *et al.*, 2024) and the role of neighbourhood size $\mathcal{N}$ as a measure of genetic drift. It predicts that in particular when $\mathcal{N}$ is low, increasing dispersal will facilitate adaptation *via* an increase in $\mathcal{N}$ - even when the total population size stays the same (and may be large). Neighbourhood size $\mathcal{N}$ can be estimated from ecological parameters of local density and disper-

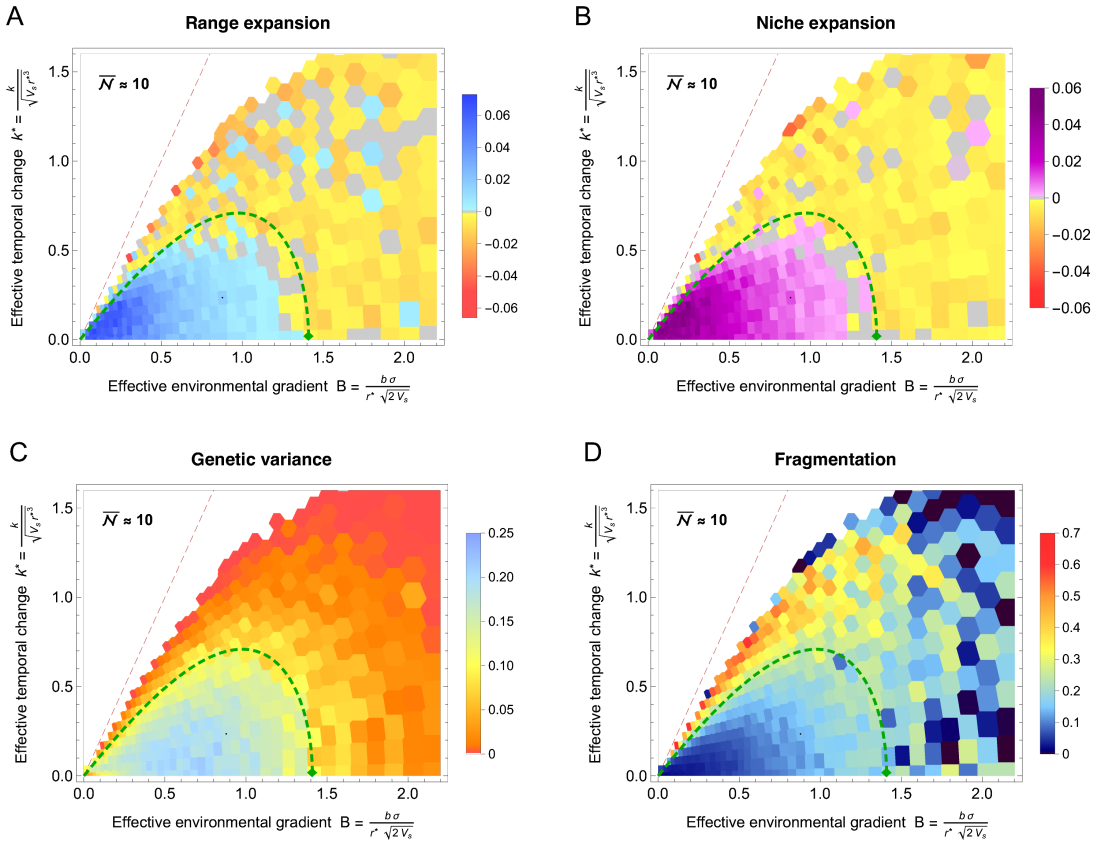

Figure 1: **Coevolution of species' range, niche and local genetic variance.** Top row: species' range (**A**) and niche (**B**) expand when sufficient variance (**A, C**) is maintained by the gene flow across the environmental gradient and contracts otherwise. The rate of range expansion is shown in blue hues and given relative to the initial range size, the rate of niche expansion is shown in purple. The rates of range and niche contraction are given in orange and red hues, while grey depicts populations showing no significant change (the 95% CI overlaps zero) and white space represents populations which went extinct within 500 generations. Each rectangle represents an independent simulation, ran across an array of changing environmental gradients b and rates of temporal change k. The expansion threshold is shown in a green dashed curve, approximated by $k_c^* = 2B(1 - 8/\mathcal{N})\sqrt{1 - (6.3B + 0.56)(\sqrt{2}B + 2h^2)/(2h^2\mathcal{N})}$. It changes both with the effective environmental gradient B and with the neighbourhood size $\mathcal{N}$. Genetic variance (**C**) initially increases with both spatial and temporal variability but collapses abruptly at the expansion threshold as the effect of genetic drift becomes too strong. (**D**): Species' range tends to fragment abruptly as the rate of temporal change increases: fragmented populations have diminished connectivity despite continuous distribution of the habitat and thus exhibit low genetic variance and high demographic stochasticity. The subsequent decline in fragmentation for steep gradients B and collapsing populations just means there is only one or two subpopulations left. Fragmentation is measured as the proportion of unoccupied space within a species range. More details, including transects and the dependency on neighbourhood size, are explained in Figs 3; while Fig. 2 supports the estimation of variance in the presence of genetic drift. Parameters: dispersal per generation $\sigma^2 = 1/2$, width of stabilising selection $V_s = 1$, maximum growth rate $r_m = 1.2$, maximum local carrying capacity $K = 6$, mutation rate $\mu = 10^{-5}$, number of loci $n_l = 1000$. Initially, 1/3 of all loci form clines which contribute to the adaptation to the environmental gradient so that in the central part of the range, trait mean matches the environmental optimum. Allelic effects are exponentially distributed with mean $\alpha = 0.07$; the mean strength of selection per locus is then $s = \alpha^2/(2V_s) \approx 0.005$. The habitat is wide enough $nd \geq 600$ so that species' range does not reach the edges along the dimension of spatial change and that the random processes (genetic drift) occur in truly two-dimensional habitat: along the neutral dimension, the number of demes is $ndy = 100$. Burn-in time (no temporal change) is 200 generations; run time 500 generations. Median neighbourhood size $\overline{\mathcal{N}} = 2\pi\sigma^2 N \approx 10$ ranges between 7 and 17 (and is higher for lower B and k^*, where the overall demographic load is lower); median total population size is about $2 \cdot 10^3$ for all surviving populations, ranging from 300 for expanding populations to $3 \cdot 10^5$ at $T = 500$ generations.

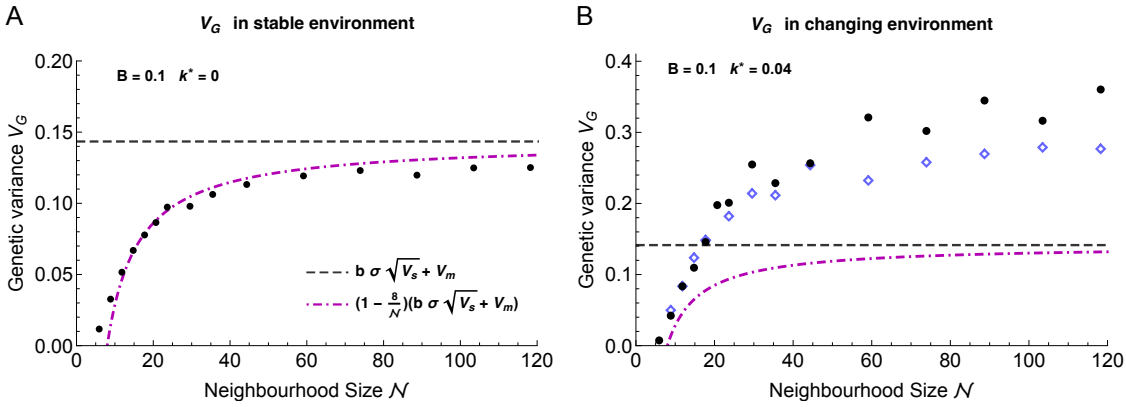

Figure 2: **Genetic variance increases with neighbourhood size $\mathcal{N} = 2\pi\sigma^2 N$, as the effect of genetic drift decreases with $1/\mathcal{N}$.** (**A**) In two-dimensional habitats, the decrease of genetic variance with drift can be desribed as $V_G \approx V_{G,det}(1 - 8/\mathcal{N})$ – shown in dash-dotted magenta. Deterministic variance (dashed gray line) is given by $V_{G,det} = b\,\sigma\sqrt{V_s} + V_m$ (Barton, 2001); where the mutational variance is $V_m = 2\mu\, n_l V_s$ and n_l gives the number of loci. (**B**) When environment changes in time, genetic variance can increase substantially as new selected alleles spread through the population. The expectations under $k^* = 0$ are given for a reference. Parameters as in Fig. 1, with burn-in time T=100 and run time T = 300 generations (see Fig. 3 **D** for temporal dynamics). Local carrying capacity ranges from $K = 2$ to $K = 50$. Black dots: neutral habitat width is fixed to $ndy = 100$; total population size thus ranges from $N_{tot} = 7 \cdot 10^3$ to $N_{tot} = 5 \cdot 10^5$. Blue open diamonds show simulations where the total population size is scaled to be approximately constant across simulations, $N_{tot} \approx 1.5 \cdot 10^5$ *via* scaling the neutral habitat width inversely with carrying capacity: $ndy = 600/K$. Habitat width set to $ndy \gtrapprox 100$ ensures that the dispersal is two-dimensional; in case the neutral habitat is considerable narrower, genetic variance becomes diminished even for high $\mathcal{N}$. This is expected because in one-dimensional habitats, neighbourhood size $\mathcal{N}_{1D} = 2\sqrt{\pi}N\sigma$ (Wright, 1943) and the effect of strength of genetic drift scales with $1/(\sqrt{s}\mathcal{N}_{1D})$ (Nagylaki, 1978a; Polechová & Barton, 2011, 2015).

sal as well as from population-genetic parameters, namely from the rate of increase in F_{ST} with distance (Rousset, 1997); for estimates and further discussion, see (Alberto *et al.*, 2005; Vekemans & Hardy, 2004). The demographic load parameters, the effective rates of spatial and temporal change (B and k), can be measured as fitness costs using transplant experiments (Burt, 2000; Polechová *et al.*, 2009).

There is an urgent need for a predictive theory to forecast adaptive responses and population resilience in changing environments (Nadeau & Urban, 2019; Urban *et al.*, 2024). Phenotypic models are a useful reference (Chevin *et al.*, 2010), yet the absence of evolutionary genetics not only precludes any inference based on the underlying genetics but it may also render the predictions not robust. In the species' range theory, both the effect of gene flow and possible benefits of adaptive plasticity change fundamentally in a model which incorporates population genetics. As stated by Whitlock (1996), who found that the benefits of plasticity trade off with the efficacy of selection in a single-locus model, errant conclusions may arise when evolutionary process is not considered as a whole. While adaptation typically requires changes at many loci and it is not really plausible to predict trajectories of all of them (Rudman *et al.*, 2022), predictions utilising higher-order parameters arising from fundamental population genetics (such as additive variance in the selected trait) are consistently fairly robust (Barton & Keightley, 2002; Yang *et al.*, 2010).

The expansion threshold marks a tipping point, beyond which genetic drift becomes too strong for the strength of environmental change, leading to the collapse of clinal adaptation. This may result in a gradual population decline, with the species' range contracting from the margins, or in an abrupt fragmentation of the species' range. While fragmentation due to spatial variation alone is limited to low neighbourhood sizes (Polechová, 2018), sharp increase in fragmentation is the expected outcome under fast rate of temporal change beyond the expansion threshold. Since fragmentation is associated with a loss of genetic variance in selected traits as well as increased demographic stochas-

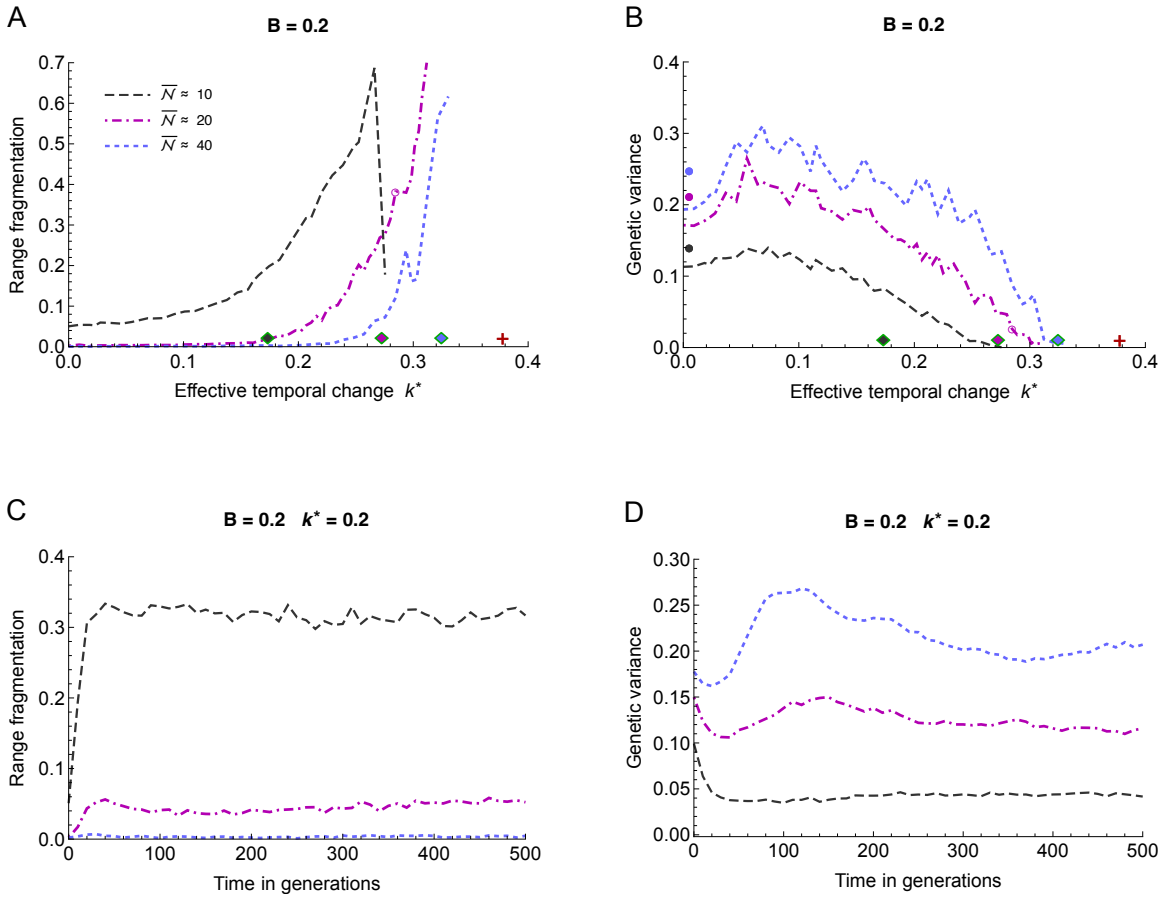

Figure 3: **Species' range can fragment abruptly when environments change through time and the neighbourhood size is small.** The increase in fragmentation (**A**) is associated with expansion threshold. The expansion threshold $k_e^*(B, \mathcal{N})$ is shown in green diamonds with colour centres matching the respective neighbourhood sizes. Beyond the expansion threshold, fragmentation occurs rapidly (**A, C**) and is accompanied by a loss of local genetic variance (**B, D**). Top row (**A, B**) shows the increasing extent of range and niche fragmentation as the effective rate of temporal change k^* increases and the neighbourhood size $\mathcal{N}$ decreases.The small circle marks an illustration shown at Fig. 4 Bottom row (**C, D**) shows the temporal dynamics where for $\overline{\mathcal{N}} \approx 10$ (black, dashed) the population is well below the expansion threshold and thus highly fragmented, for $\overline{\mathcal{N}} \approx 20$ (magenta, dot-dashed), it is just above it, and for $\overline{\mathcal{N}} \approx 40$ the population is well above the expansion threshold and thus there is no fragmentation. The neighbourhood sizes correspond to local carrying capacities $K = 5, 10, 20$, and are only slightly reduced from the maximum attainable neighbourhood size $\mathcal{N} = 2\pi\sigma^2 K$ because the dispersal load $B = 0.2$ is moderately small. Parameters as in Fig. 1. The small dots in (**B**) show the predicted genetic variance in the presence of genetic drift but for stable spatial gradients ($k^* = 0$).

ticity, recovery would be hindered even if conditions later improve.

While this theory predicts a rise in range fragmentation under temporal change (and in general at the range margins, especially on steepening gradients), it makes no claims about an abundant center (Martin *et al.*, 2024; Sagarin & Gaines, 2002): with local (Gaussian) dispersal, the eco-evolutionary dynamics dynamics is determined over local scales. Hence, carrying capacity variation over larger distances does not have a significant effect, and neither does the total range size (cf. Atkins & Travis (2010)). In reality, dispersal is rarely just local (diffusive); I have shown in that the results are qualitatively robust to a minor proportion of long-distance dispersers. However, the dynamics would be very different if the population approaches panmixia. The theory does not require spatial gradients to be linear: as the dynamics are driven at local scales, it also applies to other forms of gradual change, such as steepening

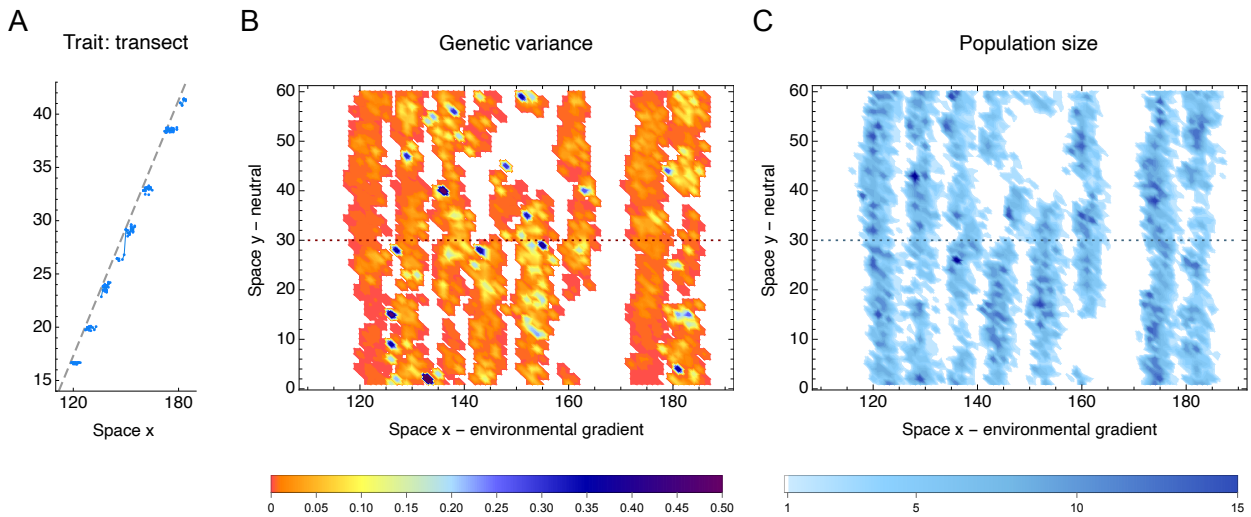

Figure 4: **Example of species' range fragmentation due to a fast temporal change** (**A**) In fragmented populations, trait mean (blue) no longer tracks the optimum (grey dashed line), each subpopulation is well adapted to a single optimum (dots: trait values; line: trait mean). This figure shows a transect at the central neutral habitat ($y = 30$). (**B**) Genetic variance is depleted, considerably below the expected value of $V_G \approx (b\,\sigma\sqrt{V_s} + V_m)(1 - 8/\mathcal{N}) = 0.21$ yet with local spikes. There is only limited gene flow across the dimension with environmental gradient (x) – in contrast, gene flow across the neutral habitat (y) is unrestricted. (**C**) The maximum population size is around carrying capacity $K = 10$ or even a little above, yet 40% of the space is unoccupied and the population gradually contracts over time. Lack of variance implies that there is almost no adaptation to the changing optimum: the population survives by tracking its optimum through space. Parameters as in Fig. 3 (**A, B**) with $k^* = 0.285$ – as shown by a small circle there. The example is chosen only slightly beyond the expansion threshold $k_c^*(B, \mathcal{N}) \approx 0.273$, where some clines in allele frequencies still persist, and thus variance is not uniformly low. The dynamics of fragmentation is illustrated in a supplementary video which shows that the fragmentation is abrupt and follows a marked increase in lag (and thus the lag load) behind the moving optimum.

gradients. (Angert *et al.*, 2020; Bridle *et al.*, 2019; Connallon & Sgrò, 2018; Polechová, 2018).

There are three major limitations to this theory. First, it considers a single trait under stabilising selection in the absence of rigid genetic trade-off, which could further limit adaptation (Heblack *et al.*, 2024). Second, it considers gradual change in continuous environments. In reality, the environment may be patchy and selection fluctuates through time, with extremes potentially incurring higher fitness costs than the steady change. Both of these complications will tend to make adaptation harder (Botero *et al.*, 2015; Gilbert & Whitlock, 2017). Third, the theory is for a single focal species. Although the environmental optimum can include both abiotic and biotic components (Case & Taper, 2000), the theory neglects the evolution of species' interactions over similar time scales (Bridle & Hoffmann, 2022). While none of these concerns invalidate the scale-free parameters, they imply that the numerical value of the expansion threshold should be considered an approximate baseline, rather than a definitive value.

Conservation genetics has been increasingly incorporated into conservation practice, and a decline in heterozygozity or effective population size N_e would be a clear cause for concern (Willi *et al.*, 2022). Yet, the utility of any cut-off value for effective population size N_e remains contested (Flather *et al.*, 2011; Frankham, 2005; Jamieson & Allendorf, 2012; Lande, 1988). At the same time, assisted migration (Aitken & Whitlock, 2013; Sexton *et al.*, 2024) is increasingly advocated to facilitate adaptation under climate change. Until now, there has not been a comprehensive predictive theory that incorporates the effect of gene flow across variable environments on local polygenic adaptation and species' range dynamics under temporal change. This theory provides a foundation for predicting when an increase in local migration is likely to be beneficial and outlines a critical threshold, beyond which the population may collapse or fragment abruptly.

Methods

The model is of evolution of a species' range in two dimensions, where both population dynamics and evolution (at many additive loci) are considered jointly. The eco-evo coupling is *via* the mean fitness $\overline{r}(\overline{z}, N)$, which gives the growth rate of the population, and decreases with increasing maladaptation: $\overline{r}(\overline{z}, N) = r_e(N) + \overline{r}_g(\overline{z})$. The ecological component of growth rate, r_e, can take various forms: here, the regulation is logistic, so that fitness declines linearly with density N: $r_e = r_m(1-N/K)$, where r_m is the maximum per capita growth rate in the limit of the local population density $N \to 0$. The carrying capacity K (for a perfectly adapted phenotype) is assumed uniform across space. The second term, $r_g(\overline{z}) \leq 0$, is the reduction in growth rate due to deviation from the optimum.

Selection is stabilising: the optimum $\theta = b\,x - kt$ changes smoothly (with a gradient b) along one spatial dimension (x), and through time t at a constant rate k. For any individual with a trait value of z, the drop in fitness due to maladaptation is $r_g(z) = -(z-\theta)^2/(2V_s)$. Here V_s gives the width of stabilising selection; strength of stabilising selection is $\gamma = -V_P/(2V_s)$, where $V_P = V_G + V_E$ is the phenotypic variance. A population with mean phenotype $\overline{z}$ has its fitness reduced by $\overline{r}_g(\overline{z}) = -(\overline{z}-\theta)^2/(2V_s) - V_P/(2V_s)$. The phenotype z is determined by many di-allelic loci with allelic effects α_i; the model is haploid, hence $\overline{z} = \sum_i \alpha_i p_i$, where p_i is the allele frequency at locus i. Phenotypic variance is $V_P = V_G + V_E$. The loss of fitness due to environmental variance V_E can be included in $r_m^* = r_m - V_E/(2V_s)$; V_E is a redundant parameter (and thus is set to zero throughout). Selection is *hard*: both the mean fitness (growth rate) and the attainable equilibrium density $\hat{N} = Kr^*/r_m = K(1 - V_P/(2r_m V_s))$ decrease with maladaptation. Expected genetic variance maintained by gene flow in the absence of genetic drift is $V_G = b\,\sigma V_s$ (Barton, 2001); the contribution due to mutation is small, at mutation-section balance $V_{G,\mu/s} = 2\mu V_s n_l$, where μ gives the mutation rate per locus and n_l the number of loci.

Evolution of trait mean with joint population dynamics; unscaled

For any given additive genetic variance V_G (assuming a Gaussian distribution of breeding values), the change in the trait mean $\overline{z}$ over time satisfies:

$$\frac{\partial \overline{z}}{\partial t} = \frac{\sigma^2}{2}\left(\frac{\partial^2 \overline{z}}{\partial x^2} + \frac{\partial^2 \overline{z}}{\partial y^2}\right) + \sigma^2\left(\frac{\partial^2 \ln(N)}{\partial x}\frac{\partial \overline{z}}{\partial x} + \frac{\partial^2 \ln(N)}{\partial y}\frac{\partial \overline{z}}{\partial y}\right) + V_G\frac{\partial \overline{r}}{\partial \overline{z}} + \zeta \tag{1}$$

The first term gives the change in the trait mean due to migration with mean displacement of σ; the second term describes the effect of the asymmetric flow from areas of higher density. The third term gives the change due to selection, given by the product of genetic variance and gradient in mean fitness (Pease *et al.*, 1989, Eq. 2). The last term ζ gives the fluctuations in the trait variance due to genetic drift: $\zeta = \sqrt{V_{G,LE}/N}\,dW_\zeta(x, y, t)$, where dW_* represents white noise in space and time (Barton *et al.*, 2002; Nagylaki, 1978b). $V_{G,LE} = \sum_i \alpha_i^2 p_i q_i$ denotes genetic variance assuming linkage equilibrium. Note that the diffusion approximation breaks down over very local scales in two dimensions because in a continuous two-dimensional habitat, two independent Brownian motions will, with probability one, never be in the same place at the same time (and thus, there would be no coalescence). The simulation avoids this problem by considering a discrete lattice, analytical approach would require introduction of a local scale of population interactions (Barton *et al.*, 2002).

The trait mean is $\overline{z} = \sum_i \alpha_i p_i$ for a haploid model, where p_i is the i-th allele frequency, $q_i = 1 - p_i$ and α_i is the effect of the allele on the trait – the change of the trait mean $\overline{z}$ as frequency of locus i changes from 0 to 1. For both haploid and diploid models, the allele frequencies p_i change as:

$$\frac{\partial p_i}{\partial t} = \frac{\sigma^2}{2}(\frac{\partial^2 p_i}{\partial x^2} + \frac{\partial^2 p_i}{\partial y^2}) + \sigma^2(\frac{\partial p_i}{\partial x}\frac{\partial \ln(N)}{\partial x} + \frac{\partial p_i}{\partial y}\frac{\partial \ln(N)}{\partial y}) + p_i q_i \frac{\partial \overline{r}}{\partial p_i} - \mu(p_i - q_i) + \epsilon \tag{2}$$

The expected change of allele frequency due to a gradient in fitness and local heterozygosity is $p_i q_i \frac{\partial \overline{r}}{\partial p_i} = s_i\, p_i q_i (p_i - q_i - 2\Delta_i)$, where selection at locus i is $s_i \equiv \alpha_i^2/(2V_s)$ and $\Delta_i = (\overline{z} - bx)/\alpha_i$ (Barton, 2001, Appendix 3). Here, the fourth term describes the change due to (symmetric) mutation at rate μ. The last term ϵ describes genetic drift (Barton *et al.*, 2002, Eq. 7): $\epsilon = \sqrt{\frac{p_i q_i}{N}}\, dW_\epsilon(x, y, t)$; where N is the haploid population density.

Population dynamics reflect diffusive migration in two dimensions, growth due to the mean Malthusian fitness $\overline{r}$, and stochastic fluctuations. The number of offspring follows a Poisson distribution with mean and variance of N, fluctuations in population numbers are given by Lande *et al.* (2003): $\xi = \sqrt{N}\, dW_\xi(x, y, t)$:

$$\frac{\partial N}{\partial t} = \frac{\sigma^2}{2}(\frac{\partial^2 N}{\partial x^2} + \frac{\partial^2 N}{\partial y^2}) + \overline{r}N + \xi \tag{3}$$

Rescaling and formalising in terms of allele frequencies, with evolution of variance

The model can be simplified by rescaling time t relative to the strength of density dependence r^*, distance x relative to dispersal σ, trait z relative to strength of stabilising selection $1/(2V_s)$ and local population size N relative to equilibrium population size with perfect adaptation: $\hat{N} = Kr^*/r_m,\ T = r^* t,\ X = x\sqrt{\frac{2r^*}{\sigma^2}},\ Z = \frac{z}{\sqrt{r^* V_s}},\ \tilde{N} = N/\hat{N}$. Note that near the equilibrium of a well-adapted population, $\tilde{N} \approx 1$.

Assuming linkage equilibrium, the rescaled equations for evolution of allele frequencies and for demographic dynamics are:

$$\begin{aligned}
\frac{\partial \tilde{N}}{\partial T} &= \frac{\partial^2 \tilde{N}}{\partial X^2} + \frac{\partial^2 \tilde{N}}{\partial Y^2} + \overline{R}\tilde{N} + \sqrt{\frac{2\tilde{N}}{\hat{N}\sigma^2}}\, dW_{\tilde{\xi}(X,Y,T)} \\
\frac{\partial p_i}{\partial T} &= \frac{\partial^2 p_i}{\partial X^2} + \frac{\partial^2 p_i}{\partial Y^2} + 2(\frac{\partial p_i}{\partial X}\frac{\partial \ln(\tilde{N})}{\partial X} + \frac{\partial p_i}{\partial Y}\frac{\partial \ln(\tilde{N})}{\partial Y}) + \\
&+ \frac{s}{r^*}(p_i q_i - 2\frac{\overline{Z} - BX - k^* T}{\alpha^*}) - \frac{\mu}{r^*}(p_i - q_i) + \sqrt{\frac{pq}{\tilde{N}\hat{N}\sigma^2}}\, dW_{\tilde{\epsilon}(X,Y,T)}
\end{aligned} \tag{4}$$

where

$$\overline{R} \equiv \overline{r}/r^* = 1 - \tilde{N} - (BX - k^* T - Z)^2/2. \tag{5}$$

The rescaled equations 4 and 5 show that four parameters fully describe the system. First, the effective rate of temporal change, $k^* = k\,/\sqrt{V_s\, r^{*3}}$. Second, the effective environmental gradient, $B \equiv b\sigma/(r^* \sqrt{2V_s})$. Third, the strength of genetic drift $1/\hat{\mathcal{N}} = 1/(2\pi\hat{N}\sigma^2)$. The parameter $\hat{\mathcal{N}}$ gives the neighbourhood size at an equilibrium with *uniform adaptation*. The fourth parameter is the strength of selection relative to the strength density dependence, s/r^*; the scaled effect of a single substitution α^* also scales with s/r^*: $\alpha^* \equiv \alpha/\sqrt{r^* V_s} = \sqrt{2s/r^*}$. The effect of this fourth parameter s/r^* is expected to be small, because typically, $s \lll r^*$. The fifth parameter, μ/r^*, will typically be very small, and will be neglected throughout. Table 1 (top) summarises the full set that describes the system.

Acknowledgements

This research was funded by the Austrian Science Fund (FWF), project doi: 10.55776/P32896, Institutional Identifier: 501100002428, grant number: P32896. The computational results were achieved using the Vienna Scientific Cluster (VSC). I would like to thank Nick Barton, Roger Butlin, Louise Fouqueau and Richard Nichols for insightful discussions over the earlier drafts.

Table 1: **Five scale-free parameters: B, k*, $\mathcal{N}$, s/r* and μ/r* describe the system**. Middle section gives informative derived parameters. The fifth parameter, scaled mutation rate μ/r^*, can be neglected because variance maintained by mutation-selection balance, $V_{G,\mu/s} = 2\mu V_s n_l$, is typically much smaller than variance generated by gene flow across environments, $V_G = b\,\sigma\,\sqrt{V_s}$. The middle column gives the dimensions of the parameters, where T stands for time, D for distance and Z for trait.

param.	dim.	description
k^*	–	effective rate of temporal change $k^* = k\,/\,\sqrt{V_s\,r^{*3}}$
B	–	effective environmental gradient $B = b\sigma/(r^*\,\sqrt{2V_s})$
$\mathcal{N}$	–	neighbourhood size $\mathcal{N} = 4\pi N_e\sigma^2 = 2\pi N\sigma^2$
s/r^*	–	strength of selection per locus relative to the strength of density-dependence
s	$1/T$	selection per locus: $s \equiv \alpha^2/(2V_s)$
r^*	$1/T$	rate of return to equilibrium pop. size: $r^* \equiv -N\,\partial\bar{r}/\partial N\|_{N\to\hat{N}} = r_m - V_G/(2V_s)$
b	Z/D	gradient in the environmental optimum
V_s	Z^2T	variance of stabilising selection
σ	$D/\sqrt{T}$	dispersal per generation
K	T/D^2	max. carrying capacity (haploid) K = N when all phenotypes are perfectly adapted
r_m	$1/T$	max. intrinsic rate of increase
α	Z	allelic effect
μ	$1/T$	mutation rate, $\mu \equiv 10^{-5}$

References

Aguilée, R., Raoul, G., Rousset, F. & Ronce, O. (2016). Pollen dispersal slows geographical range shift and accelerates ecological niche shift under climate change. *Proceedings of the National Academy of Sciences*, 113, E5741–E5748.

Aitken, S.N. & Whitlock, M.C. (2013). Assisted gene flow to facilitate local adaptation to climate change. *Annual Review of Ecology, Evolution, and Systematics*, 44.

Alberto, F., Gouveia, L., Arnaud-Haond, S., Pérez-Lloréns, J.L., Duarte, C.M. & Serrão, E.A. (2005). Within-population spatial genetic structure, neighbourhood size and clonal subrange in the seagrass *Cymodocea nodosa*. *Molecular Ecology*, 14, 2669–2681.

Alberto, F.J., Aitken, S.N., Alía, R., González-Martínez, S.C., Hänninen, H., Kremer, A., Lefèvre, F., Lenormand, T., Yeaman, S., Whetten, R. *et al.* (2013). Potential for evolutionary responses to climate change–evidence from tree populations. *Global change biology*, 19, 1645–1661.

Angert, A.L., Bontrager, M.G. & Ågren, J. (2020). What do we really know about adaptation at range edges? *Annual Review of Ecology, Evolution, and Systematics*, 51, 341–361.

Atkins, K. & Travis, J. (2010). Local adaptation and the evolution of species' ranges under climate change. *Journal of Theoretical Biology*, 266, 449–457.

Barton, N. (2001). Adaptation at the edge of a species' range. In: *Integrating ecology and evolution in a spatial context* (eds. Silvertown, J. & Antonovics, J.). Blackwell, vol. 14, pp. 365–392.

Barton, N., Depaulis, F. & Etheridge, A. (2002). Neutral evolution in spatially continuous populations. *Theoretical Population Biology*, 61, 31–48.

Barton, N. & Keightley, P. (2002). Understanding quantitative genetic variation. *Nature reviews genetics*, 3, 11–21.

Benning, J.W., Hufbauer, R.A. & Weiss-Lehman, C. (2022). Increasing temporal variance leads to stable species range limits. *Proceedings of the Royal Society B*, 289, 20220202.

Botero, C.A., Weissing, F.J., Wright, J. & Rubenstein, D.R. (2015). Evolutionary tipping points in the capacity to adapt to environmental change. *Proceedings of the National Academy of Sciences*, 112, 184–189.

Bridle, J. & Hoffmann, A. (2022). Understanding the biology of species' ranges: when and how does evolution change the rules of ecological engagement? *Philosophical Transactions of the Royal Society B*, 377, 20210027.

Bridle, J.R., Kawata, M. & Butlin, R.K. (2019). Local adaptation stops where ecological gradients steepen or are interrupted. *Evolutionary Applications*, 12, 1449–1462.

Burt, A. (2000). Natural selection in the wild. *Trends in Ecology & Evolution*, 15, 306–307.

Case, T. & Taper, M. (2000). Interspecific competition, environmental gradients, gene flow, and the coevolution of species' borders. *The American Naturalist*, 155, 583–605.

Charlesworth, B., Charlesworth, D. & Barton, N.H. (2003). The effects of genetic and geographic structure on neutral variation. *Annual Review of Ecology, Evolution, and Systematics*, 34, 99–125.

Chevin, L.M., Lande, R. & Mace, G.M. (2010). Adaptation, plasticity, and extinction in a changing environment: towards a predictive theory. *PLoS Biology*, 8, e1000357.

Christiansen, F.B. (1975). Hard and soft selection in a subdivided population. *American Naturalist*, 109, 11–16.

Connallon, T. & Sgrò, C.M. (2018). In search of a general theory of species' range evolution. *PLoS Biology*, 16, e2006735.

Czuppon, P., Blanquart, F., Uecker, H. & Débarre, F. (2021). The effect of habitat choice on evolutionary rescue in subdivided populations. *The American Naturalist*, 197, 625–643.

Débarre, F., Ronce, O. & Gandon, S. (2013). Quantifying the effects of migration and mutation on adaptation and demography in spatially heterogeneous environments. *Journal of Evolutionary Biology*, 26, 1185–1202.

Felsenstein, J. (1976). The theoretical population genetics of variable selection and migration. *Annual review of genetics*, 10, 253–280.

Fisher, R. (1930). *The genetical theory of natural selection*. Clarendon Press.

Flather, C.H., Hayward, G.D., Beissinger, S.R. & Stephens, P.A. (2011). Minimum viable populations: is there a 'magic number'for conservation practitioners? *Trends in ecology & evolution*, 26, 307–316.

Fouqueau, L. & Polechová, J. (2024). Eco-evolutionary dynamics in changing environments: integrating theory with data. *Journal of Evolutionary Biology*, 37, 579–587.

Frankham, R. (2005). Genetics and extinction. *Biological conservation*, 126, 131–140.

Garcia Castillo, D., Barton, N., Faria, R., Larsson, J., Stankowski, S., Butlin, R., Johannesson, K. & Westram, A.M. (2024). Predicting rapid adaptation in time from adaptation in space: a 30-year field experiment in marine snails. *Science Advances*, 10, eadp2102.

Gilbert, K.J. & Whitlock, M.C. (2017). The genetics of adaptation to discrete heterogeneous environments: frequent mutation or large-effect alleles can allow range expansion. *Journal of evolutionary biology*, 30, 591–602.

Gomulkiewicz, R. & Holt, R.D. (1995). When does evolution by natural selection prevent extinction? *Evolution*, pp. 201–207.

Haldane, J.B.S. (1956). The relation between density regulation and natural selection. *Proceedings of the Royal Society of London, B: Biological Sciences*, 145, 306–308.

Haldane, J.B.S. (1957). The cost of natural selection. *Journal of Genetics*, 55, 511–524.

Heblack, J., Schepers, J.R. & Willi, Y. (2024). Reduced evolutionary potential under heat and drought stress at the southern range edge of north american *Arabidopsis lyrata*. *Journal of Evolutionary Biology*, p. voae045.

Hedrick, P.W. (1986). Genetic polymorphism in heterogeneous environments: a decade later. *Annual review of ecology and systematics*, pp. 535–566.

Holt, R.D., Barfield, M. & Gomulkiewicz, R. (2004). Temporal variation can facilitate niche evolution in harsh sink environments. *The American Naturalist*, 164, 187–200.

Holt, R.D., Barfield, M. & Peniston, J.H. (2022). Temporal variation may have diverse impacts on range limits. *Philosophical Transactions of the Royal Society B*, 377, 20210016.

Holt, R.D. & Gomulkiewicz, R. (1997). How does immigration influence local adaptation? a reexamination of a familiar paradigm. *The American Naturalist*, 149, 563–572.

Jamieson, I.G. & Allendorf, F.W. (2012). How does the 50/500 rule apply to mvps? *Trends in ecology & evolution*, 27, 578–584.

King, J.G. & Hadfield, J.D. (2019). The evolution of phenotypic plasticity when environments fluctuate in time and space. *Evolution letters*, 3, 15–27.

Kirkpatrick, M. & Barton, N. (1997). Evolution of a species' range. *The American Naturalist*, 150, 1–23.

Lande, R. (1976). Natural selection and random genetic drift in phenotypic evolution. *Evolution*, 30, 314–334.

Lande, R. (1988). Genetics and demography in biological conservation. *Science*, 241, 1455–1460.

Lande, R., Barrowclough, G.F. *et al.* (1987). Effective population size, genetic variation, and their use in population management. In: *Viable populations for conservation* (ed. Soulé, M.E.). Cambridge University Press, pp. 87–124.

Lande, R., Engen, S. & Sæther, B.E. (2003). *Stochastic population dynamics in ecology and conservation*. Oxford University Press.

Lande, R. & Shannon, S. (1996). The role of genetic variation in adaptation and population persistence in a changing environment. *Evolution*, 50, 434–437.

Martin, P.R., Robinson, O.J. & Bonier, F. (2024). Rare edges and abundant cores: range-wide variation in abundance in north american birds. *Proceedings of the Royal Society B*, 291, 20231760.

Nadeau, C.P. & Urban, M.C. (2019). Eco-evolution on the edge during climate change. *Ecography*, 42, 1280–1297.

Nagylaki, T. (1978a). A diffusion model for geographically structured populations. *Journal of Mathematical Biology*, 6, 375–382.

Nagylaki, T. (1978b). Random genetic drift in a cline. *Proceedings of the National Academy of Sciences of the United States of America*, 75, 423–426.

Osmond, M.M. & Klausmeier, C.A. (2017). An evolutionary tipping point in a changing environment. *Evolution*, 71, 2930–2941.

Paixão, T. & Barton, N.H. (2016). The effect of gene interactions on the long-term response to selection. *Proceedings of the National Academy of Sciences*, 113, 4422–4427.

Pease, C., Lande, R. & Bull, J. (1989). A model of population growth, dispersal and evolution in a changing environment. *Ecology*, 70, 1657–1664.

Polechová, J. (2018). Is the sky the limit? On the expansion threshold of a species' range. *PLoS biology*, 16, e2005372.

Polechová, J. & Barton, N. (2011). Genetic drift widens the expected cline but narrows the expected cline width. *Genetics*, 1, 227–235.

Polechová, J. & Barton, N. (2015). Limits to adaptation along environmental gradients. *Proceedings of the National Academy of Sciences of the United States of America*, 112, 6401–6406.

Polechová, J., Barton, N. & Marion, G. (2009). Species' range: Adaptation in space and time. *The American Naturalist*, 174, E186–204.

Ronce, O. & Kirkpatrick, M. (2001). When sources become sinks: migrational meldown in heterogeneous habitats. *Evolution*, 55, 1520–1531.

Rousset, F. (1997). Genetic differentiation and estimation of gene flow from f-statistics under isolation by distance. *Genetics*, 145, 1219–1228.

Rudman, S.M., Greenblum, S.I., Rajpurohit, S., Betancourt, N.J., Hanna, J., Tilk, S., Yokoyama, T., Petrov, D.A. & Schmidt, P. (2022). Direct observation of adaptive tracking on ecological time scales in drosophila. *Science*, 375, eabj7484.

Sagarin, R.D. & Gaines, S.D. (2002). The 'abundant centre' distribution: to what extent is it a biogeographical rule? *Ecology Letters*, 5, 137–147.

Sexton, J., Clemens, M., Hall, J. & Hoffmann, A. (2024). Patterns and effects of gene flow on adaptation across spatial scales: implications for management and models. *Journal of Evolutionary Biology*, 37, 732–745.

Sexton, J., McIntyre, P., Angert, A. & Rice, K. (2009). Evolution and ecology of species range limits. *Annual Review of Ecology, Evolution, and Systematics*, 40, 415–436.

Tomasini, M. & Peischl, S. (2022). The role of spatial structure in multi-deme models of evolutionary rescue. *Journal of evolutionary biology*, 35, 986–1001.

Uecker, H., Otto, S.P. & Hermisson, J. (2014). Evolutionary rescue in structured populations. *The American Naturalist*, 183, E17–E35.

Urban, M.C., Swaegers, J., Stoks, R., Snook, R.R., Otto, S.P., Noble, D.W., Moiron, M., Hällfors, M.H., Gómez-Llano, M., Fior, S. *et al.* (2024). When and how can we predict adaptive responses to climate change? *Evolution Letters*, 8, 172–187.

Vekemans, X. & Hardy, O.J. (2004). New insights from fine-scale spatial genetic structure analyses in plant populations. *Molecular ecology*, 13, 921–935.

Whitlock, M.C. (1996). The red queen beats the jack-of-all-trades: the limitations on the evolution of phenotypic plasticity and niche breadth. *The American Naturalist*, 148, S65–S77.

Willi, Y., Kristensen, T.N., Sgrò, C.M., Weeks, A.R., Ørsted, M. & Hoffmann, A.A. (2022). Conservation genetics as a management tool: The five best-supported paradigms to assist the management of threatened species. *Proceedings of the National Academy of Sciences*, 119, e2105076119.

Wright, S. (1943). Isolation by distance. *Genetics*, 28, 114 – 138.

Wright, S. (1946). Isolation by distance under diverse systems of mating. *Genetics*, 31, 39.

Wright, S. *et al.* (1932). The roles of mutation, inbreeding, crossbreeding, and selection in evolution. *Proceedings of the 6th International Congress of Genetics*, 1, 356–366.

Yang, J., Benyamin, B., McEvoy, B.P., Gordon, S., Henders, A.K., Nyholt, D.R., Madden, P.A., Heath, A.C., Martin, N.G., Montgomery, G.W. *et al.* (2010). Common snps explain a large proportion of the heritability for human height. *Nature genetics*, 42, 565–569.